

Supporting Information

**Axisymmetric Bis-Tridentate Ir(III) Photoredox Catalysts for
Anticancer Phototherapy Under Hypoxia[†]**

Li Wei,^a Rajesh Kushwaha,^b Anyi Dao,^a Zhongxian Fan,^{a,c} Samya Banerjee,^b Huaiyi Huang^{*a}

^a*School of Pharmaceutical Sciences (Shenzhen), Shenzhen Campus of Sun Yat-sen University, Sun Yat-sen University, Shenzhen 518107, P. R. China.*

^b*Indian Institute of Technology (BHU), Varanasi, 221005, India. Email: samya.chy@itbhu.ac.in (Dr. Samya Banerjee)*

^c*Shenshan Medical Center, Memorial Hospital of Sun Yat-sen university*

Contents

Experimental section

Tables

Table S1. Log $P_{o/w}$ values and phosphorescence quantum yields (Φ) of **Ir1-Ir3**

Table S2. Computed absorption energies of the complexes in DCM

Table S3. Singlet oxygen generation quantum yield (Φ_{Δ}) of **Ir1-Ir3**

Table S4. Dark- and photo-cytotoxicity of **Ir1-Ir3**

Figures

Fig. S1. ^1H NMR spectrum of **Ir1**

Fig. S2. ^1H NMR and ^1H - ^1H COSY spectrum of **Ir2**

Fig. S3. ^1H NMR and ^1H - ^1H COSY spectrum of **Ir3**

Fig. S4. ^{13}C NMR spectrum of **Ir3**

Fig. S5. HRMS spectrum of **Ir3**

Fig. S6. HPLC spectra of **Ir3**

Fig. S7. UV-Vis spectra of **Ir1-Ir3**

Fig. S8. 2D and 3D emission spectra of **Ir1-Ir3**

Fig. S9. Phosphorescence spectra of **Ir1-Ir3** in air or nitrogen-saturated CH_2Cl_2

Fig. S10. Spatial plots of selected frontier orbitals of the DFT optimized ground state of **Ir2-Ir3**

Fig. S11. UV-vis spectra to determine the light stability of **Ir1-Ir3**

Fig. S12. ^1H NMR spectra to determine the dark and light stability of **Ir3**

Fig. S13. Determination of singlet oxygen of **Ir1-Ir3** by degradation experiment of ABDA

Fig. S14. Determination of $^1\text{O}_2$ generation quantum yield of **Ir1-Ir3**

Fig. S15. Plot of the change in absorbance of ABDA at 380 nm against the irradiation time

Fig. S16. Photocatalytic oxidation of NADH by **Ir1-Ir3**

Fig. S17. Turnover numbers (TON) and turnover frequency (TOF) calculations from spectra of **Ir1-Ir3** for NADH photo-oxidation

Fig. S18. Photocatalytic reduction of oxidized Fe^{3+} -cyt c by NADH and **Ir3**

Fig. S19. Determination of $\text{O}_2^{\cdot-}$ generation of **Ir1-Ir3** by monitoring the emission spectra of DHR123

Fig. S20. Determination of $\text{O}_2^{\cdot-}$ generation Quenching by NADH by monitoring the emission spectra of DHR123 after treatment with **Ir3**

Fig. S21. Relative intracellular NADH levels of A549/DDP cells treated with **Ir3**

Fig. S22. Intracellular generation of Reactive Oxygen Species (ROS) in A549/DDP cells induced by **Ir3**

Fig. S23. Intracellular generation of Singlet Oxygen ($^1\text{O}_2$) in A549/DDP cells induced by **Ir3**

Fig. S24. Intracellular generation of superoxide radicals ($\text{O}_2^{\cdot-}$) in A549/DDP cells induced by **Ir3**

Fig. S25. Change in the mitochondrial membrane potential in A549/DDP cells induced by **Ir3**

Fig. S26. Photo-induced necro-apoptotic death of A549/DDP cells by **Ir3** from Annexin V/PI staining

References

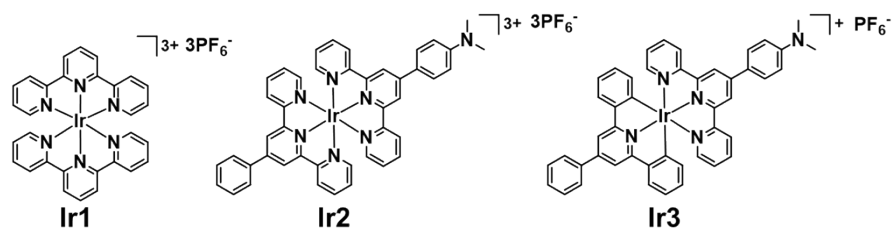
Experimental section

Materials

All reagents and materials from commercial sources. 2,2':6',2''-terpyridine, 4'-Phenyl-2,2':6',2''-terpyridine, 2,4,6-Triphenylpyridine, 4-(Dimethylamino)benzaldehyde, 2-Acetylpyridine and 9,10-anthracenediyl-bis(methylene)dimalonic acid (ABDA) were purchased from Bidepharm. Dihydrorhodamine 123 (DHR 123) was purchased from Aladdin. 3-(4,5-dimethylthiazol-2-yl)-2,5-diphenyltetrazolium bromide (MTT) was purchased from Macklin. β -Nicotinamide adenine dinucleotide, reduced disodium salt I (β -NADH) from Sigma-Aldrich. Human lung carcinoma cell line (A549), DDP-resistant human lung adenocarcinoma cell line (A549/DDP) were obtained from Procell Life Science & Technology Co., Ltd. Dulbecco Modified Eagle Medium (DMEM), fetal bovine serum (FBS), penicillin/streptomycin and phosphate buffered saline (PBS) were bought from Gibco. Mito Tracker™ Green FM, Lyso Tracker™ Green DND-26 were purchased from Life Technologies Corporation. Mitochondrial membrane potential assay kit with JC-1, Annexin V-FITC/PI Apoptosis Detection Kit, Reactive oxygen species assay kit (DCFH-DA) and Dihydroethidium (DHE) were purchased from Beyotime Biotechnology. Singlet oxygen sensor green reagent (SOSG) was purchased from meilunbio®.

Instruments

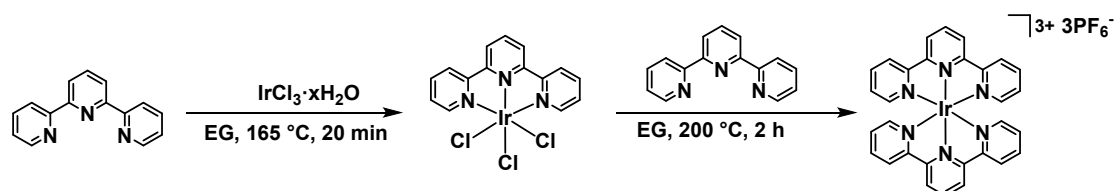
¹H NMR spectra were recorded on a Bruker AV-400 and AV-600 spectrometer. Structural assignments were made with additional information from ¹H-¹H COSY experiments. High-Resolution Mass spectra were analyzed by LCMS-IT-TOF (Shimadzu, Japan). UV-Vis spectra were recorded on a Yoke T3202S UV-Vis spectrophotometer. Emission spectra and the emission quantum yield measurements were made using a Techcomp FL970 fluorescence spectrophotometer. Confocal microscopy was visualized by laser confocal microscopy (LSM 880, Carl Zeiss, Göttingen, Germany). White light irradiation in PDT was provided by a commercially available LED visible area light source (Shenzhen Puri Materials Technologies, Co., Ltd. China).



Scheme 1. Chemical structure of Ir1-Ir3.

Synthesis and characterization

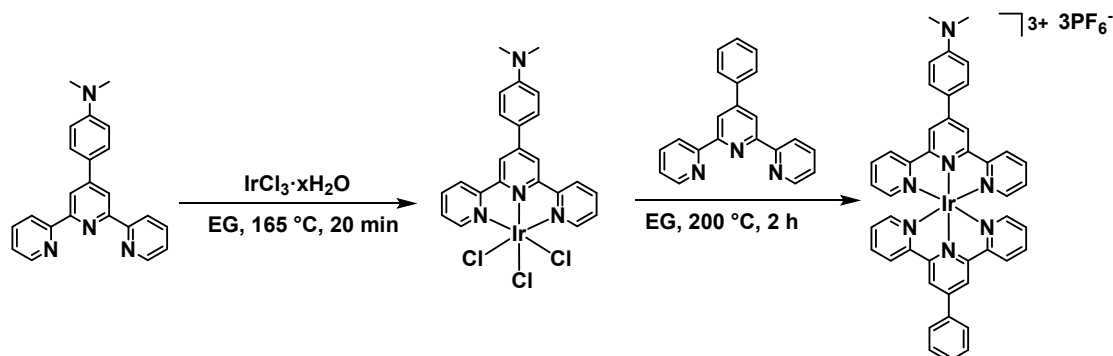
Synthesis of 4'-(p-dimethylaminophenyl)-2,2':6',2''-terpyridine (Me₂N-ph-tpy): Me₂N-ph-tpy was prepared following reported literature with moderately adapted.^[1] To a mixture of 2-Acetylpyridine (6.057 g, 50 mmol) and 4-(Dimethylamino)benzaldehyde (3.730 g, 25 mmol) was added a solution of NaOH (2.0 g) in ethanol (100 mL), and then NH₃·H₂O solutions (120 mL) was added. The mixture was stirred for 4 h at room temperature. A yellow precipitate was collected and washed with EtOH. The resulting solid was filtered and dry in vacuum. The crude product obtained was purified by column chromatography to give green powder (566 mg, 6.5%). ¹H NMR (400 MHz, CDCl₃) δ 8.76 – 8.63 (m, 6H), 7.91 – 7.81 (m, 4H), 7.33 (ddd, *J* = 7.5, 4.8, 1.2 Hz, 2H), 6.81 (d, *J* = 8.9 Hz, 2H), 3.02 (s, 6H).



Synthesis of Ir(tpy)Cl₃: 2,2':6',2''-terpyridine (187 mg, 0.8 mmol), Iridium(III) chloride hydrate (304 mg, 0.96 mmol) were dissolved in ethylene glycol (8 mL) and then were heated to 165 °C for 20 min. After the reaction, the mixture was cooled to room temperature. The solution was filtered. And the filter was washed using EtOH and then dried to give orange powder (238 mg, 56%).

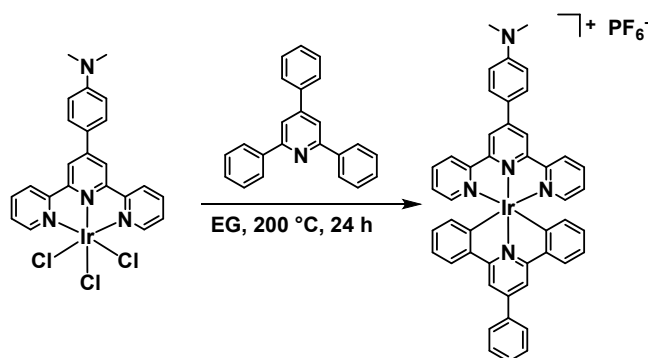
Synthesis of [Ir(tpy)₂](PF₆)₃ (Ir1): The precursor Ir(tpy)Cl₃ (106 mg, 0.2 mmol), 2,2':6',2''-terpyridine (47 mg, 0.2 mmol) were dissolved in ethylene glycol (5 mL) and then heated to 200 °C for 2 h. After the reaction, the mixture was cooled to room temperature, followed by addition of saturated ammonium hexafluorophosphate aqueous solution. The resulting precipitate was filtered

and dry under vacuum. The crude product obtained was purified by column chromatography to give orange red powder (201 mg, 92%). ESI-MS (MeOH): $[M-3PF_6]^{3+}$ calcd for $[C_{30}H_{22}IrN_6]^{3+}$: 219, found: 219. 1H NMR (400 MHz, DMSO- d_6) δ 9.22 (d, $J = 8.3$ Hz, 4H), 8.97 – 8.88 (m, 6H), 8.31 (t, $J = 7.9$ Hz, 4H), 7.80 (d, $J = 5.8$ Hz, 4H), 7.54 (t, $J = 6.8$ Hz, 4H).



Synthesis of $Ir(Me_2N-ph-tpy)Cl_3$: 4'-(p-dimethylaminophenyl)-2,2':6',2''-terpyridine (106 mg, 0.3 mmol), Iridium(III) chloride hydrate (114 mg, 0.36 mmol) were dissolved in ethylene glycol (5 mL) and then were heated to 165 °C for 20 min. After the reaction, the mixture was cooled to room temperature. The solution was filtered. And the filter was washed using EtOH and then dried to give red powder (109 mg, 56%).

Synthesis of $[Ir(Me_2N-ph-tpy)(4'-ph-tpy)](PF_6)_3$ (Ir2): The precursor $Ir(Me_2N-ph-tpy)Cl_3$ (130 mg, 0.2 mmol), 4'-ph-tpy (62 mg, 0.2 mmol) were dissolved in ethylene glycol (5 mL) and then were heated to 200 °C for 2 h. After the reaction, the mixture was cooled to room temperature, followed by addition of saturated ammonium hexafluorophosphate aqueous solution. The resulting precipitate was filtered and dry in vacuum. The crude product obtained was purified by column chromatography to give red powder (31 mg, 12%). ESI-MS (MeOH): $[M-3PF_6]^{3+}$ calcd for $[C_{44}H_{35}IrN_7]^{3+}$: 284, found: 284. 1H NMR (400 MHz, DMSO- d_6) δ 9.64 (s, 2H), 9.47 (s, 2H), 9.25 (d, $J = 8.1$ Hz, 4H), 8.50 – 8.42 (m, 4H), 8.35 (q, $J = 8.0$ Hz, 4H), 7.99 (d, $J = 4.3$ Hz, 2H), 7.93 (d, $J = 5.7$ Hz, 2H), 7.84 (t, $J = 7.5$ Hz, 2H), 7.75 (t, $J = 7.4$ Hz, 1H), 7.62 – 7.50 (m, 4H), 7.03 (d, $J = 9.1$ Hz, 2H), 3.18 (s, 6H).



Synthesis of [Ir(Me₂N-ph-tpy)(2,4,6-Triphenylpyridine)](PF₆) (Ir3): The precursor Ir(Me₂N-ph-tpy)Cl₃ (130 mg, 0.2 mmol), 2,4,6-Triphenylpyridine (62 mg, 0.2 mmol) were dissolved in ethylene glycol (5 mL) and then were heated to 200 °C for 24 h. After the reaction, the mixture was cooled to room temperature, followed by addition of saturated ammonium hexafluorophosphate aqueous solution. The resulting precipitate was filtered and dry in vacuum. The crude product obtained was purified by column chromatography to give red powder (28 mg, 14%). HR-ESI-MS (MeOH): [M-PF₆]⁺ calcd for [C₄₆H₃₅IrN₅]⁺: 850.2522, found: 850.2513. **Anal. calc. for C₄₆H₃₅F₆IrN₅P: C, 55.53; H, 3.55; N, 7.04. Found: C, 55.77; H, 3.89; N, 6.58.** ¹H NMR (600 MHz, DMSO-*d*₆) δ 9.33 (s, 2H), 9.05 (d, *J* = 8.2 Hz, 2H), 8.55 (s, 2H), 8.32 – 8.29 (m, 4H), 8.19 (d, *J* = 7.8 Hz, 2H), 8.07 (t, *J* = 7.8 Hz, 2H), 7.80 (d, *J* = 5.2 Hz, 2H), 7.71 (t, *J* = 7.6 Hz, 2H), 7.61 (t, *J* = 7.5 Hz, 1H), 7.36 (t, *J* = 6.8 Hz, 2H), 7.00 (d, *J* = 8.7 Hz, 2H), 6.96 (t, *J* = 7.6 Hz, 2H), 6.72 (t, *J* = 7.4 Hz, 2H), 6.22 (d, *J* = 7.3 Hz, 2H), 3.12 (s, 6H). ¹³C NMR (151 MHz, DMSO-*d*₆) δ 165.59, 164.61, 156.98, 151.78, 151.52, 151.37, 150.04, 147.11, 146.89, 146.39, 137.97, 137.34, 136.57, 133.19, 130.23, 129.73, 129.12, 128.74, 127.89, 127.68, 126.25, 125.21, 124.33, 124.27, 123.49, 122.26, 119.00, 118.45, 113.83, 112.18, 31.16, 29.83.

HPLC analysis

Ir3 was analyzed on an RP-HPLC column (Zorbax SB-C18 column, 4.6 × 250 mm, 5.0 μm, Agilent, USA) with isocratic elution of 0.1% aqueous formic acid (15%) and ACN (containing 0.1% formic acid, 85%); flow rate, 1.0 mL/min. The temperature of the column was ambient. **Ir3** was detected through PDA detector.

Log P_{o/w} measurement

The pre-saturated water and n-octanol mixture was obtained by shaking the mixture of water and n-

octanol for 24 h. Complexes were added to 1 mL pre-saturated n-octanol and 1 mL pre-saturated water solution, and the final concentration of the complexes was 100 μM , then the mixture was shaken overnight in the dark at room temperature. After stationary, the absorbance of the oil/water phase in acetonitrile solution was determined by a UV-Vis spectrophotometer. The partition coefficient of the complexes was calculated from the equation $\log P_{o/w} = \log (C_o/C_w)$, where C_o/C_w represents the concentration of the complexes in the octanol/water phase.

UV-Vis spectroscopy

The UV-Vis spectra were obtained with a Yoke T3202S UV-Vis spectrophotometer. The UV-Vis spectra of complexes (10 μM) in a 1-cm quartz cuvette with nine different solvents were obtained at room temperature from 900 to 250 nm. The complexes (10 μM) in the different solvents were diluted from a stock solution in DMSO (10 mM).

Fluorescence spectra

Fluorescence emission measurements were performed on a Techcomp FL970 fluorescence spectrophotometer. Complexes (10 μM) in eight different solvents were excited in a 1-cm quartz cuvette at room temperature.

Photoluminescence quantum yield^[2,3]

Photoluminescence spectra were obtained with a fluorescence spectrophotometer. The relative photoluminescence quantum yields were determined with $\text{Ru}(\text{bpy})_3\text{Cl}_2$ or Rhodamine 6G as the standard using the following equation:

$$\Phi_x = \Phi_s * (F_x/F_s) * (A_s/A_x) * (n_x/n_s)^2$$

Where Φ represents quantum yield; F stands for integrated area under the corrected emission spectrum; A is absorbance at 450 nm for $\text{Ru}(\text{bpy})_3\text{Cl}_2$ as standard and at 525 nm for Rhodamine 6G as standard, the excitation wavelength; n is the refractive index of the solution; and the subscripts x and s refer to the complex sample and the standard, respectively. Complexes were diluted from a stock solution in DMSO to achieve an absorbance = 0.1 at 450 nm in water or acetonitrile and at 525 nm in Ethanol. The Φ_s value for $\text{Ru}(\text{bpy})_3\text{Cl}_2$ in aerated water and acetonitrile at 298K were measured to be 0.04 and 0.018 respectively, and the Φ_s value for Rhodamine 6G in aerated Ethanol

at 298K were measured to be 0.95. These values for the phosphorescence quantum yield of Ru(bpy)₃Cl₂ and Rhodamine 6G have been reported in previous literatures.

Photo-stability of complexes

For the photo-stability experiment, The DMEM solution (containing 10 % fetal bovine serum and 1 % penicillin-streptomycin) of complexes (10 μM) was prepared at ambient temperature. UV-Vis spectra of that solution were recorded at room temperature every five minutes after light irradiation with white light (power: 14.3 mW/cm²). Mapping with the absorbance change of complexes vs irradiation time was done.

Computational details

The complexes were studied in their cationic form by Density Functional Theory (DFT) using the Gaussian 16 quantum chemistry package. Figure S16 represents the optimized structures and spatial plots of selected frontier orbitals of the complexes. We had used LANL2DZ basis set for Ir and 6-31g* for all other atoms with B3LYP function for geometry optimization. The geometries were evaluated in vacuum and the solvation energies were calculated using CPCM solvation model and in DCM. Restricted DFT and unrestricted DFT were used to evaluate excited state of the complexes and they were confirmed as local minimum with no imaginary frequencies. The absorption energies were computed using time-dependent (TD) formalism of DFT and employing B3LYP functional in DCM.

Singlet oxygen measurements

The singlet oxygen generation by complexes was determined using a steady-state method with ABDA as the ¹O₂ probe. The water containing the tested samples (5 μM) and ABDA (200 μM) were prepared in the dark and irradiated with white light (power: 14.3 mW/cm²) for 5 min, the absorbance from 500 to 300 nm was measured after each irradiation. Mapping with the absorbance change of ABDA vs irradiation time was done.

Singlet oxygen generation quantum yield measurements^[4]

Singlet oxygen generation quantum yields (Φ_{Δ}) of Ir1-Ir3 were determined using a steady-state

method with ABDA as the $^1\text{O}_2$ probe and $[\text{Ru}(\text{bpy})_3]\text{Cl}_2$ as the standard ($\Phi_\Delta = 0.18$ in H_2O). The solution, containing the tested complex and ABDA ($100 \mu\text{M}$) was prepared in the dark and then was irradiated with 465 nm light (power: $65 \text{ mW}/\text{cm}^2$) for 30 s. The absorbance of the solution was measured after each irradiation. The absorbance at 465 nm of the complex and $[\text{Ru}(\text{bpy})_3]\text{Cl}_2$ was kept at 0.1. Mapping with the absorbance change of ABDA at 380 nm vs irradiation time, and singlet oxygen generation quantum yields (Φ_Δ) of the complexes were calculated according to the following equation:

$$\Phi_{\Delta(x)} = \Phi_{\Delta(\text{std})} * (S_x/S_{\text{std}}) * (F_{\text{std}}/F_x)$$

where subscripts x and std designate the sample (complex) and $[\text{Ru}(\text{bpy})_3]\text{Cl}_2$, respectively; S stands for the slope of plot where time dependent absorbance of ABDA in 380 nm was plotted against the irradiation time (s). F stands for the absorption correction factor, which is given by $F = 1 - 10^{-\text{OD}}$ (OD represents the optical density of sample and $[\text{Ru}(\text{bpy})_3]\text{Cl}_2$ at irradiation wavelength).

Photocatalytic reactions of complexes with NADH^[5]

Reactions between complexes and NADH at different ratios were monitored by UV-Vis spectroscopy at room temperature in the dark or upon photo-irradiation with white light (power: $14.3 \text{ mW}/\text{cm}^2$). Turnover number (TON) is defined as the number of moles of NADH that a mole of complex can convert within 20 min. Turnover frequency (TOF) was calculated from the difference in NADH concentration after 20 min irradiation divided by the concentration of complex. The concentration of NADH was obtained using the extinction coefficient $\epsilon_{339} = 6220 \text{ M}^{-1} \cdot \text{cm}^{-1}$.

Photocatalytic reduction of Fe^{3+} -cyt c by Ir3 and NADH^[5]

Photocatalytic reduction of oxidized Fe^{3+} -cyt c ($11.2 \mu\text{M}$) by Ir3 ($5 \mu\text{M}$) in the presence or absence of NADH ($50 \mu\text{M}$) was studied by UV-vis spectroscopy at 298 K in the dark or on irradiation with white light ($14.3 \text{ mW}/\text{cm}^2$) under aerated or deaerated condition. About the deaerated operation, the PBS solution was degassed by sonication for 10 min followed by purging with Ar for 20 min. Stock solutions of Fe^{3+} -cyt c (10 mM in PBS), NADH (10 mM in PBS) and Ir3 (10 mM in DMSO) were added under Ar atmosphere.

Cell culture

Cell lines A549, A549/DDP were maintained in DMEM medium supplemented with 10% fetal bovine serum, and 1% penicillin-streptomycin solution. All cells were grown at 310 K in a humidified incubator which provided an atmosphere of 5% CO₂/95% air (Thermo Fisher). After cell attachment, the cells for hypoxic treatment were transferred to an hypoxic incubator in a biological safety cabinet within a glove box (Defendor HW1000, Hariolab) at 310 K, 5% O₂, 5% CO₂ and 90% N₂ for another 8 h allowing the cells to adapt to hypoxic conditions.

Cell viability assay

Cytotoxicities of the tested complexes were determined by the MTT assay. Cells were seeded in 96-well flat-bottomed microplates (ca. 5000 cells/well) in a growth medium (100 µL) and incubated at 37 °C in a 5% CO₂/95% incubator for 24 h. Then fresh medium containing different concentrations of the complexes was added to each well for 4 h, and changed with fresh medium for 44 h. Wells containing untreated cells were used as blank controls. To test the photo-toxicity of the complexes, cells were incubated with complexes for 4 h under normoxia (5% CO₂/95% air) or hypoxia (5% O₂, 5% CO₂ and 90% N₂) and then changed with fresh medium, followed by light irradiation (white light: 17.2 J/cm²), and then incubation was continued for another 44 h. Then, MTT in PBS (10 µL, 5 mg/mL) was added to each well and incubated for another 4 h at 37 °C. After that, the medium was removed and DMSO (100 µL) was added to each well to dissolve the formed purple formazan. The absorbance of the solutions at 595 nm was measured with an Epoch™ Microplate Spectrophotometer (BioTek). The IC₅₀ values for the complexes were determined from the dose dependence cell survival curve. This experiment was repeated triplicates.

Cellular localization assay

A549/DDP cells were seeded in 35 mm glass-bottom dishes (Corning) and allowed to adhere for 48 h. The cells were then incubated with Ir3 (1 µM) at 37 °C for 2 h and then further co-incubated with the commercial lysosomal probe LTDR (100 nM) or mitochondrial probe MTR (100 nM) for an additional 30 min. The cells were washed with PBS once and visualized by using an LSM 880 laser confocal microscope (Carl Zeiss, Germany) immediately with a 40× objective lens. Ir3 was excited at 488 nm, Lyso- and Mito- Tracker were excited at 488 nm. The phosphorescence/fluorescence was collected at 680 ± 80 nm for Ir3 and 550 ± 40 nm for Lyso- and Mito-Tracker.

Intracellular Reactive Oxygen Species (ROS) detection

A549/DDP cells were seeded at a density of 5000 cells/well of a 96-well plate for 48 h. Then, the cells were incubated with **Ir3** for 2 h, followed by light irradiation (white light: 17.2 J/cm²). After that, cells were stained with 10 μM of DCFH-DA (ROS probe) for 30 min, and then the fluorescence images were immediately captured using a fluorescence microscope.

A549/DDP cells were seeded at a density of 5000 cells/well of a 6-well plate for 48 h. Then, the cells were incubated with **Ir3** for 2 h, followed by light irradiation (white light: 17.2 J/cm²). After that, cells were stained with 10 μM of DCFH-DA (ROS probe) for 30 min, and after Cell Harvesting, the fluorescence intensity was immediately analyzed using a Flow cytometer (Beckman counter).

Intracellular O₂^{•-} detection

A549/DDP cells were seeded at a density of 5000 cells/well of a 96-well plate for 48 h. Then, the cells were incubated with **Ir3** for 2 h, followed by light irradiation (white light: 17.2 J/cm²). After that, the dihydroethidium (DHE, O₂^{•-} specific probe, 10 μM) was added and then incubated for 30 min at 37 °C. The fluorescence images were immediately acquired with a fluorescence microscope.

Determination of intracellular singlet oxygen (¹O₂)

A549/DDP cells were seeded at a density of 5000 cells/well of a 96-well plate for 48 h. Then, the cells were incubated with **Ir3** for 2 h, followed by light irradiation (white light: 17.2 J/cm²). After that, the Singlet Oxygen Sensor Green Reagent (SOSG, ¹O₂ specific probe, 10 μM) was added and then incubated for 30 min at 37 °C. The fluorescence images were immediately acquired with a fluorescence microscope.

Detection of intracellular NADH level

A549/DDP cells were seeded at a density of 5000 cells/well of a 6-well plate for 48 h. Then, the cells were incubated with **Ir3** for 2 h, followed by light irradiation (white light: 17.2 J/cm²). After that, the NAD⁺/NADH Assay product (Beyotime Biotechnology) was used to measure the intracellular NADH level. The absorbance was recorded using a microplate reader. Three replicates were set for each sample, and the standard deviations were calculated in each group.

Detection of mitochondrial membrane potential

Change in the mitochondrial membrane potential was monitored by JC-1 assay. Briefly, A549/DDP cells were seeded at a density of 5000 cells/well of a 96-well plate for 48 h. The cells were incubated with **Ir3** for 2 h, and then irradiated with light (white light: 17.2 J/cm²). The JC-1 was added and

then incubated for 30 min at 37 °C. Then cells were washed once with PBS, followed by the imaging using a fluorescence microscope.

Annexin V-FITC/PI assay

Annexin V-FITC staining of the membranes was performed by using the annexin V-FITC and PI apoptosis detection kit. A549/DDP cells were incubated with **Ir3** for 2 h and then irradiated with a LED lamp (white light: 17.2 J/cm²). After removing the medium, the cells were stained with annexin V-FITC (2.5 µL) and PI (5 µL) for 20 min. Then, the fluorescence images were obtained using a fluorescence microscope.

Table**Table S1.** Log $P_{o/w}$ values phosphorescence quantum yields (Φ) of Ir(III) complexes.

| Complexes | Log $P_{o/w}$ | Φ | | |
|------------|------------------------|-------------------------------|---------------------------------|-------------------|
| | | H ₂ O ^a | CH ₃ CN ^a | EtOH ^b |
| Ir1 | -0.33 ^{±0.02} | n. a. | n. a. | n. a. |
| Ir2 | -0.44 ^{±0.01} | n. a. | n. a. | n. a. |
| Ir3 | +0.26 ^{±0.01} | 0.010 | 0.003 | 0.009 |

^aEmission quantum yields (Φ) of complexes in H₂O and CH₃CN. [Ru(bpy)₃]Cl₂ was used as standard excitation with 450 nm light;

^bEmission quantum yields (Φ) of complexes in EtOH. Rhodamine 6G was used as standard excitation with 525 nm light.

n. a. = not available.

Table S2. Computed absorption energies of the complexes in CH₂Cl₂.

| | Adsorption Energy | E (eV) | f ^a |
|------------|--------------------------------|--------|----------------|
| Ir2 | S ₀ -S ₁ | 1.20 | - |
| | S ₀ -S ₂ | 1.54 | 0.0005 |
| | S ₀ -S ₃ | 1.61 | 0.0038 |
| Ir3 | S ₀ -S ₁ | 2.03 | 0.0132 |
| | S ₀ -S ₂ | 2.20 | 0.2946 |
| | S ₀ -S ₃ | 2.28 | 0.0051 |

^aOscillator Strength. Determination of oscillator strengths of singlet \leftrightarrow triplet transitions is beyond the scope of the theory used.

Table S3. Singlet oxygen generation quantum yield (Φ_{Δ}) of **Ir1-Ir3** in aqueous solution.

| Complex | Ir1 | Ir2 | Ir3 | Ru(bpy)₃Cl₂ |
|-----------------|------------|------------|------------|--|
| Φ_{Δ} | n. a. | 0.014 | 0.055 | 0.18 |

Ru(bpy)₃]Cl₂ was used as the standard.

n. a. = not available due to extremely low light absorption at 465 nm.

Table S4. Dark- and photo-cytotoxicity of Ir1-Ir3.

| Cell Line | A549 | | | A549/DDP | | | |
|-----------|-------------------|--------------------|---------------------|-------------------|--------------------|---------------------|--------|
| | Dark ^a | Light ^b | PI ^c | Dark ^a | Light ^b | PI ^c | |
| Normoxia | Ir1 | >100 | >100 | n. a. | >100 | >100 | n. a. |
| | Ir2 | 98.6 \pm 4.8 | 49.3 \pm 0.74 | 2.00 | >100 | 79.8 \pm 1.94 | >1.2 |
| | Ir3 | 0.80 \pm 0.05 | 0.0012 \pm 0.0002 | 666.7 | 3.03 \pm 0.14 | 0.0033 \pm 0.0003 | 918.1 |
| | DDP ^d | 2.80 \pm 0.12 | - | - | 37.98 \pm 0.88 | - | - |
| Hypoxia | Ir3 | 3.85 \pm 1.08 | 0.028 \pm 0.004 | 137.5 | 9.39 \pm 0.68 | 0.0082 \pm 0.0005 | 1145.1 |
| | DDP ^d | 3.58 \pm 0.25 | - | - | 69.23 \pm 1.24 | - | - |

Cell cytotoxicity tests were repeated triplicates. ^a4 h drug exposure in the dark, replaced by fresh medium and followed by 44 h incubation. ^b4 h drug exposure in the dark, replaced by fresh medium and white light irradiation (17.2 J/cm²) followed by 44 h incubation. ^cPI = IC₅₀(Dark)/IC₅₀(Light). ^d48 h drug exposure.

Figures

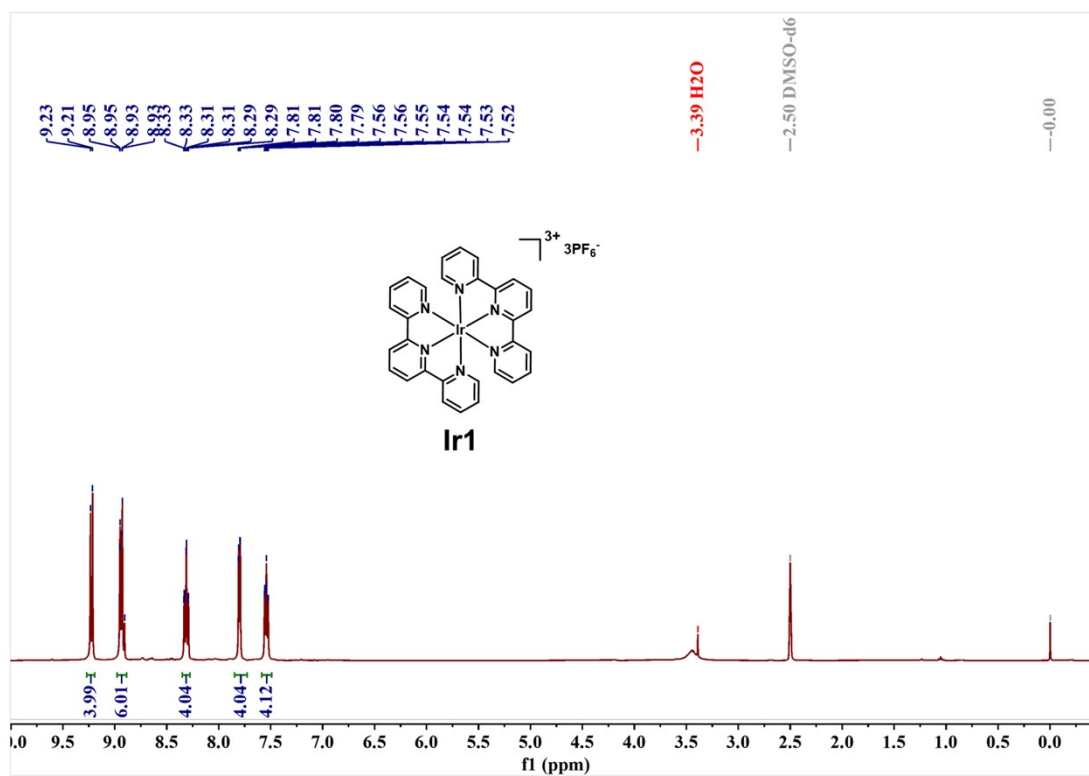


Fig. S1. ^1H NMR spectrum of **Ir1** in $\text{DMSO-}d_6$.

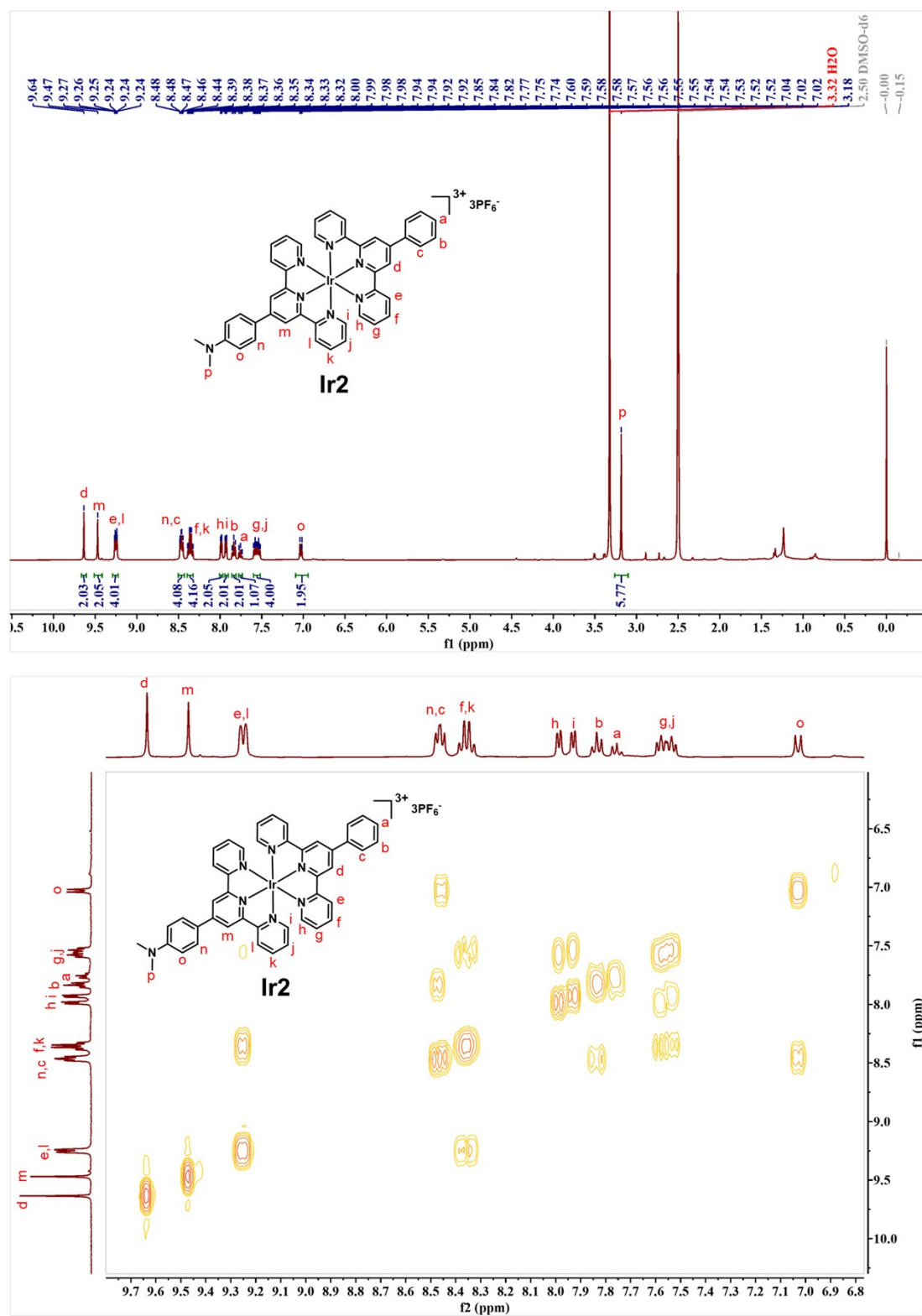


Fig. S2. ^1H NMR and ^1H - ^1H COSY spectrum of **Ir2** in $\text{DMSO-}d_6$.

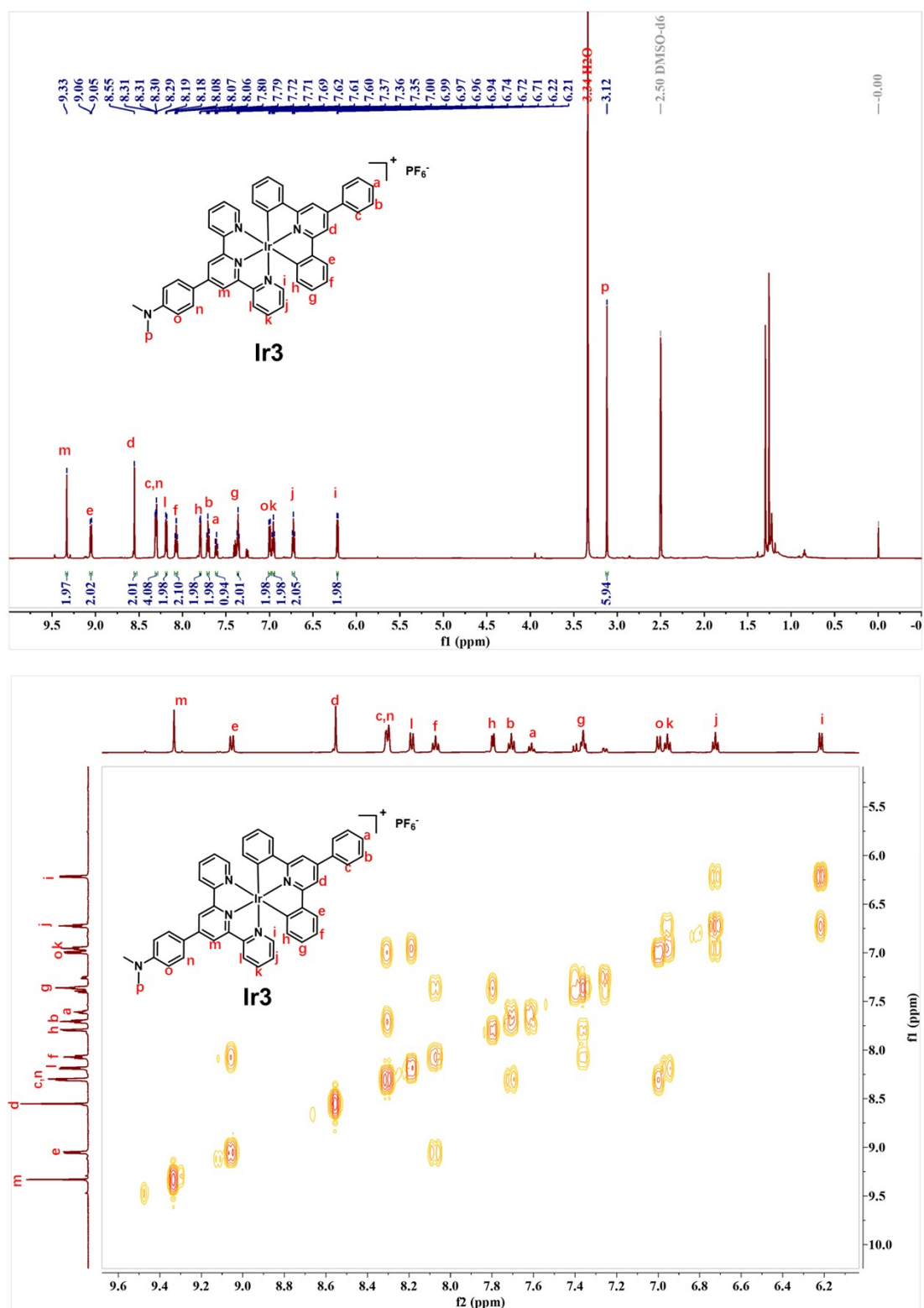


Fig. S3. ^1H NMR and ^1H - ^1H COSY spectrum of **Ir3** in $\text{DMSO-}d_6$.

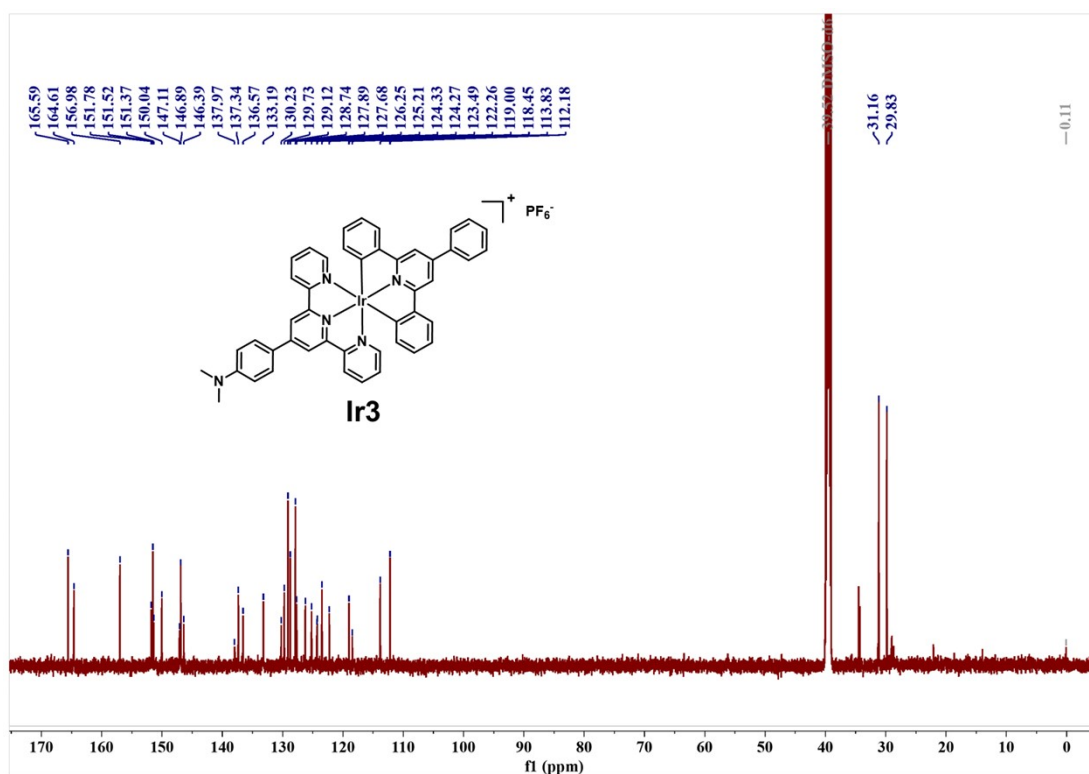


Fig. S4. ^{13}C NMR spectrum of **Ir3** in $\text{DMSO-}d_6$.

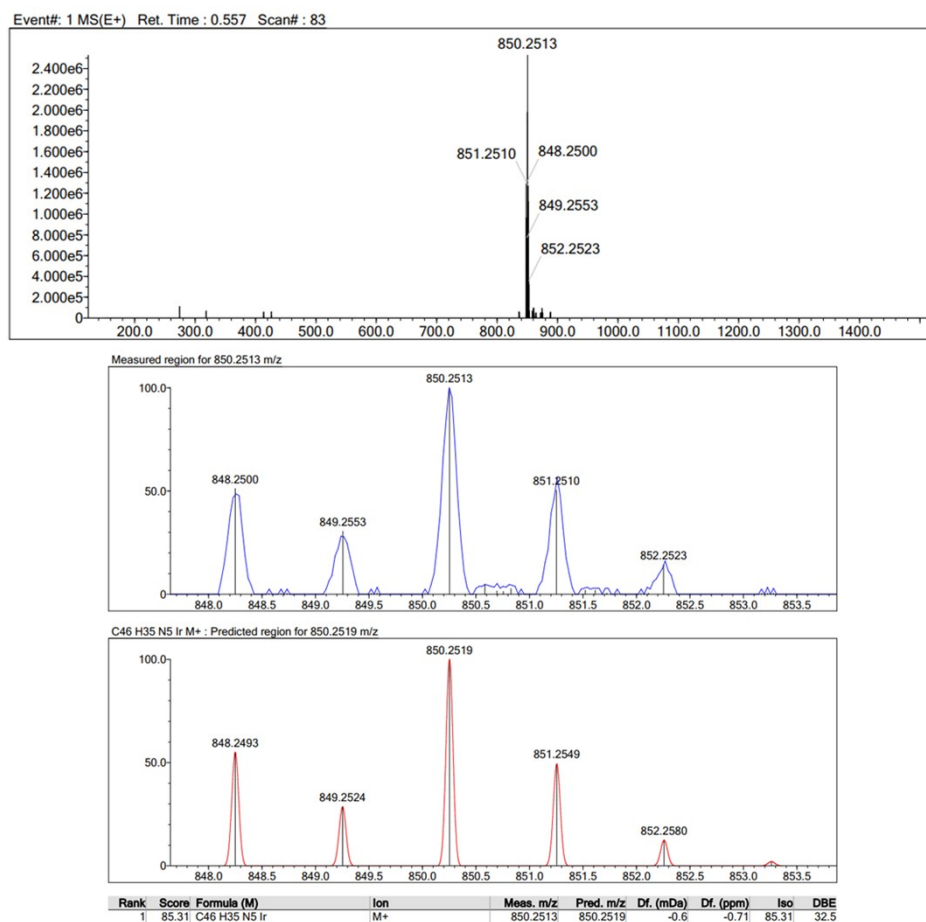


Fig. S5. HRMS spectrum of **Ir3** in MeOH.

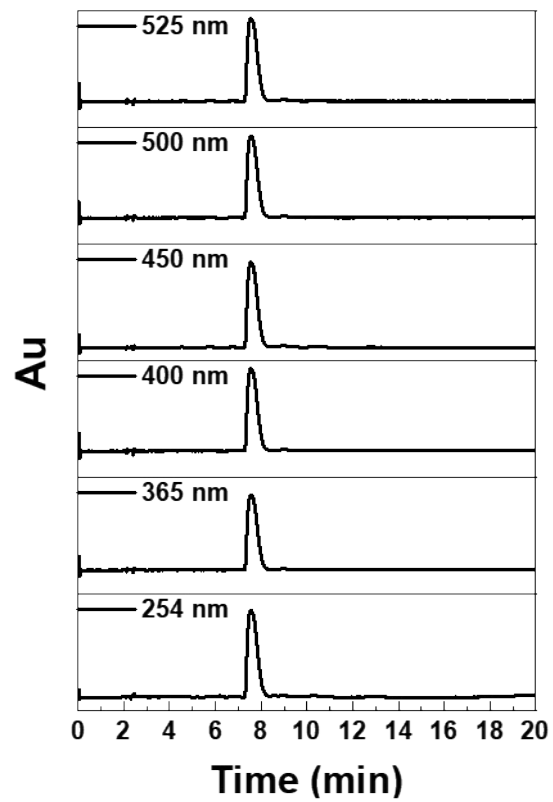


Fig. S6. HPLC spectra of Ir3.

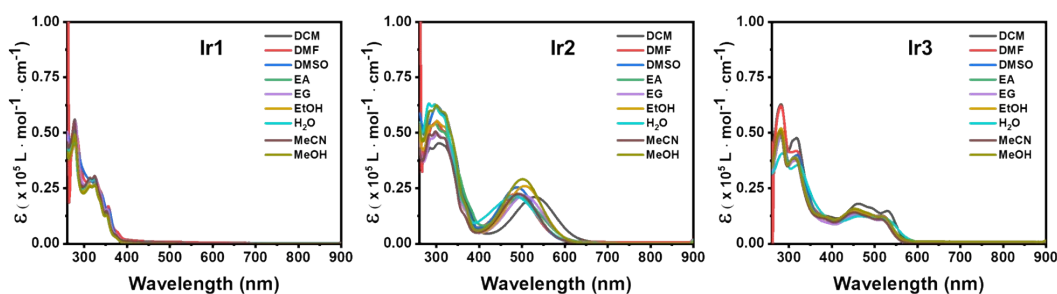


Fig. S7. UV-Vis absorption (all 10 μM) of the complexes in various solvents at room temperature.

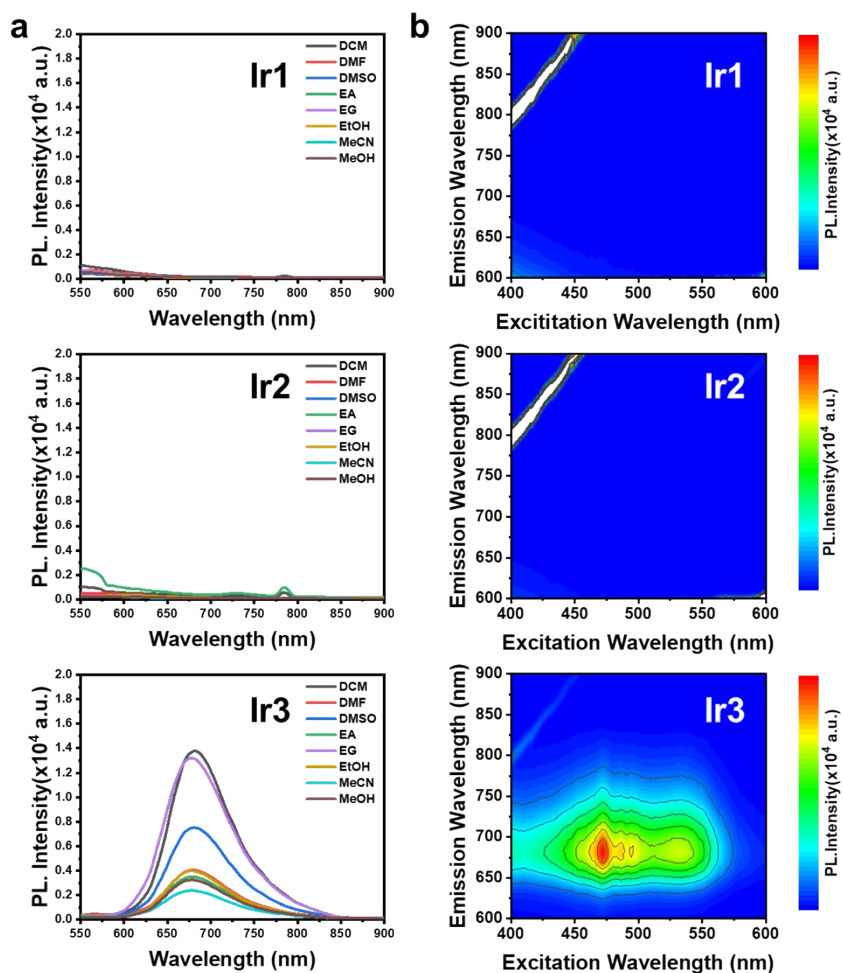


Fig. S8. (a) Emission spectra of the complexes (all 10 μM , $\text{Ex}=525\text{ nm}$) in various solvents at room temperature. (b) 3D mapping fluorescence spectra of the complexes (all 10 μM) in dichloromethane at room temperature.

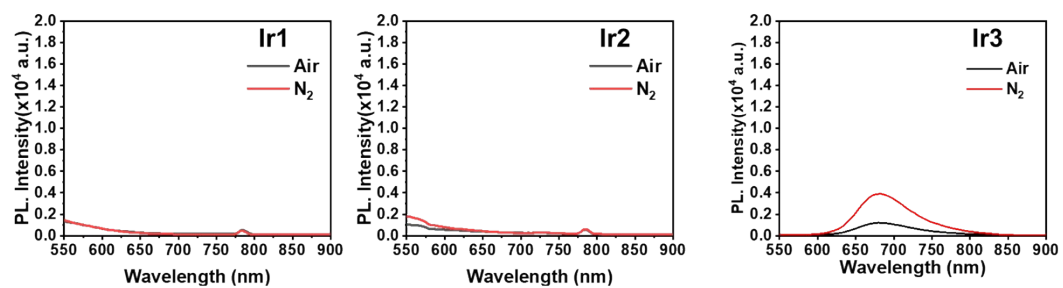


Fig. S9. Emission spectra of the complexes (all 5 μ M) in dichloromethane at Air saturated and N_2 saturated.

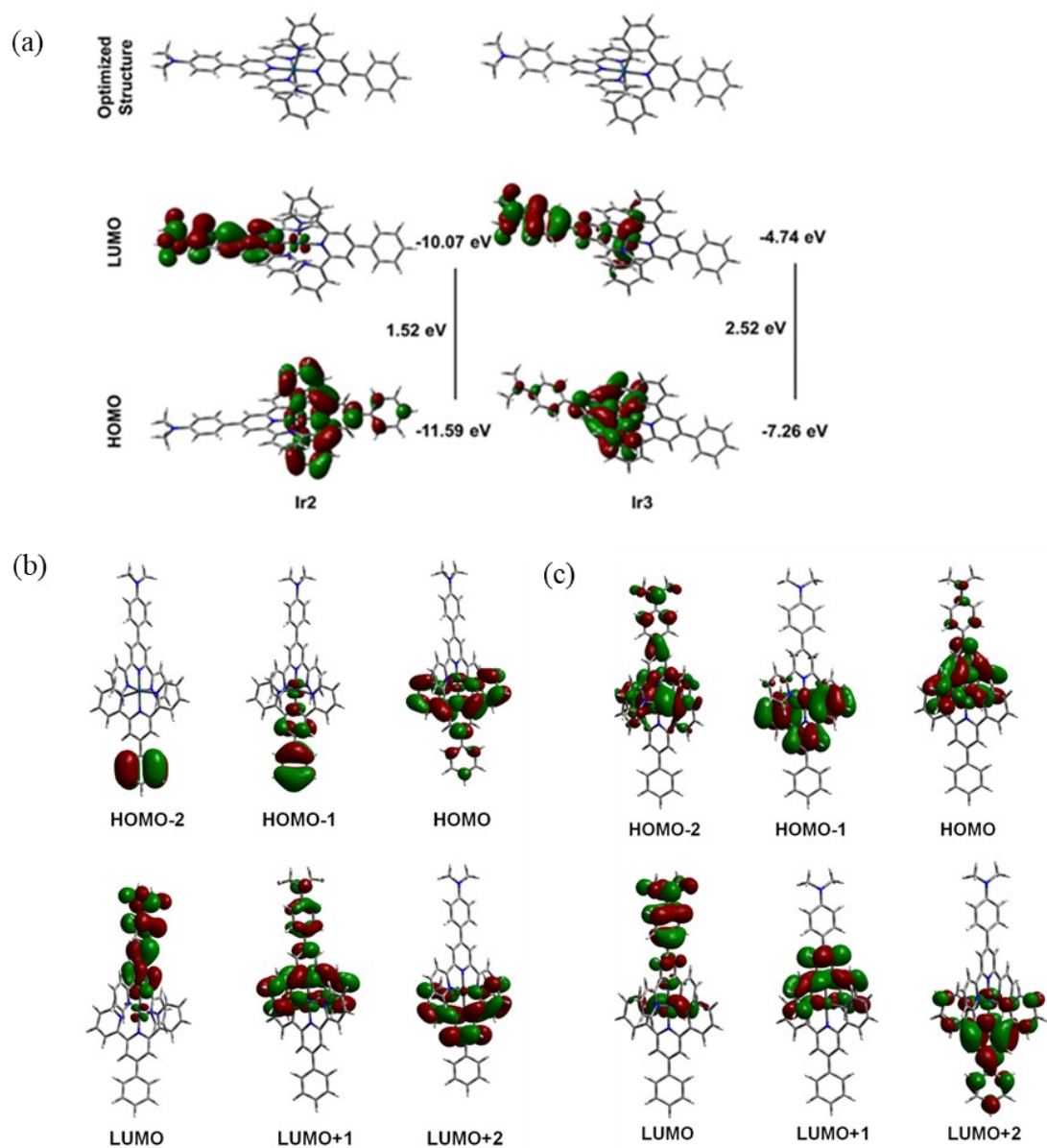


Fig. S10. (a) Energy-optimized structures and frontier molecular orbitals of the complexes **Ir2** and **Ir3**. Colour codes: Iridium, sky-blue; nitrogen, dark blue; carbon, grey; and hydrogen, white. (b) Spatial plots of selected frontier orbitals of the DFT optimized ground state of complex **Ir2**. (c) Spatial plots of selected frontier orbitals of the DFT optimized ground state of complex **Ir3**.

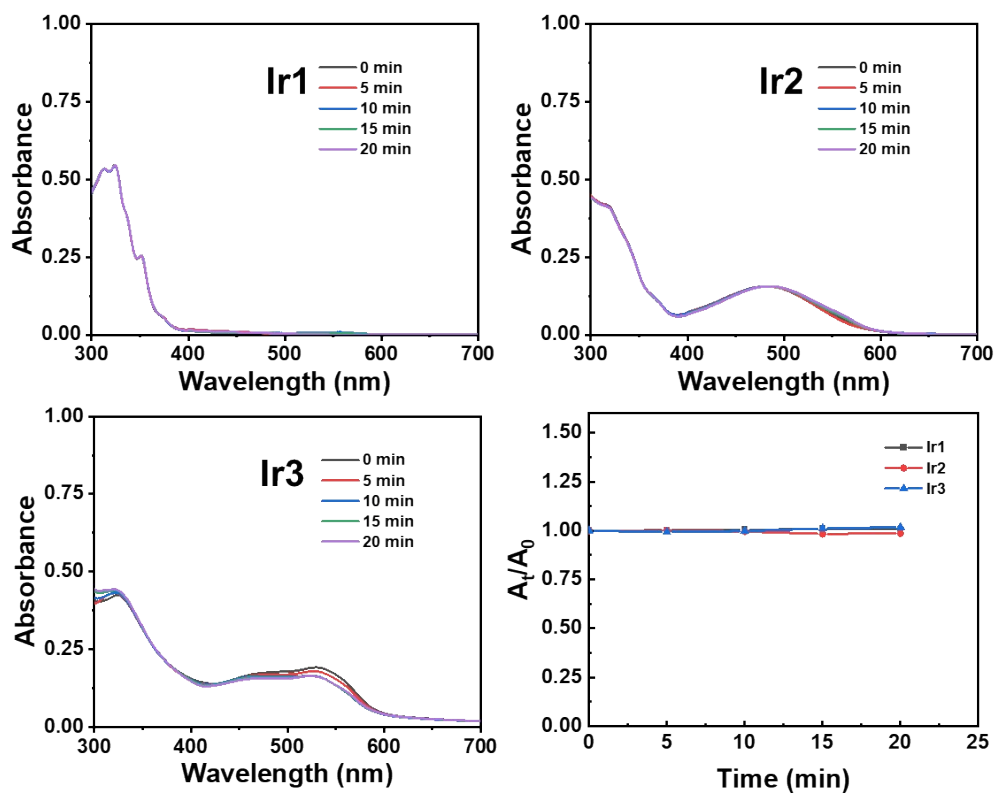


Fig. S11. Photo-stability of **Ir1-Ir3** (10 μ M) in DMEM (containing 10 % fetal bovine serum and 1 % penicillin-streptomycin) as was evaluated by time-dependent UV-Vis spectroscopy. Light used: white light LED lamp (irradiance: 14.3 mW/cm²). The absorbance at 390 nm was selected to compared the A_t/A_0 of **Ir1-Ir3**.

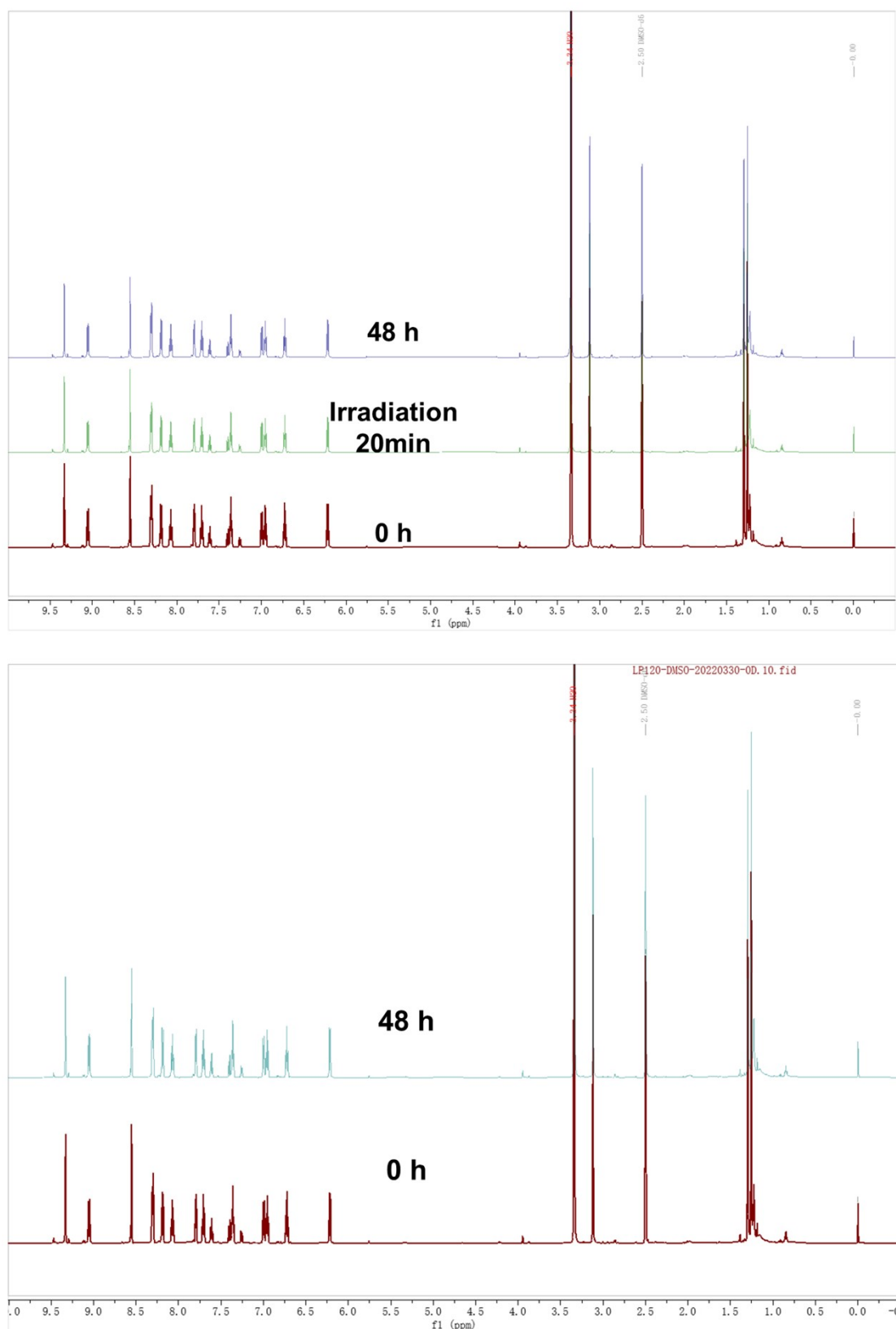


Fig. S12. Photo- and dark-stability of **Ir3** in $\text{DMSO-}d_6$ as was evaluated by ^1H NMR. Top: White light LED lamp (irradiance: $14.3 \text{ mW}/\text{cm}^2$). Bottom: Dark.

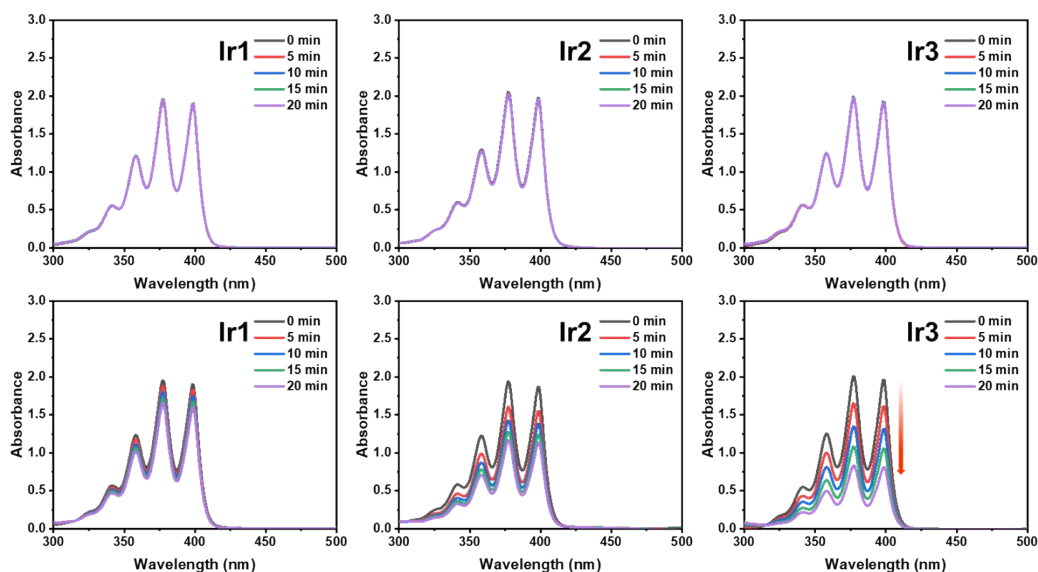


Fig. S13. Determination of $^1\text{O}_2$ generation by complexes via monitoring the time-dependent UV-Vis absorption spectra of ABDA ($200\ \mu\text{M}$) after treatment with complexes ($5\ \mu\text{M}$). Top: Dark. Bottom: White light LED lamp (irradiance: $14.3\ \text{mW}/\text{cm}^2$).

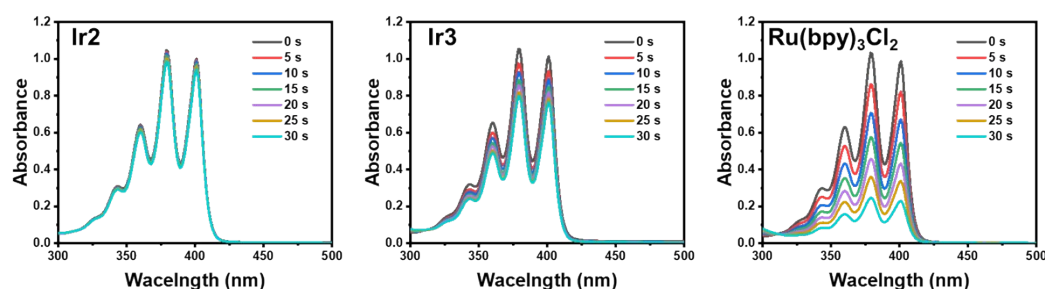


Fig. S14. Determination of $^1\text{O}_2$ generation quantum yield of Ir2-Ir3 by monitoring the time-dependent UV-vis absorption spectra of ABDA after treatment with Ir2-Ir3 or $[\text{Ru}(\text{bpy})_3]\text{Cl}_2$ standard ($\text{OD}_{465\ \text{nm}} = 0.1$). Conditions: $465\ \text{nm}$ LED lamp (irradiance: $65\ \text{mW}/\text{cm}^2$).

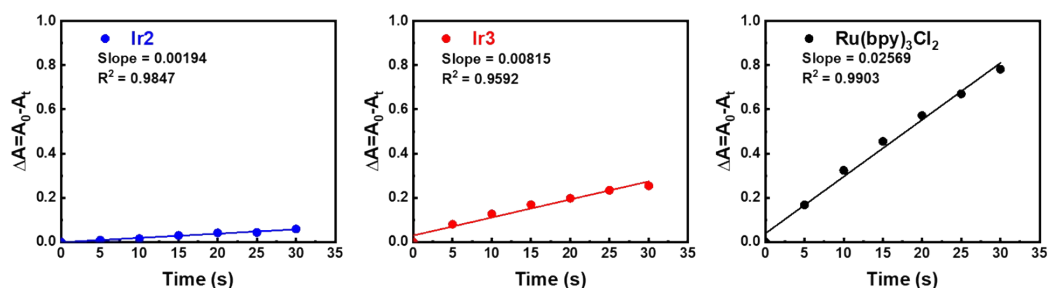


Fig. S15. Plot of the change in absorbance of ABDA at $380\ \text{nm}$ against the irradiation time (s). Conditions: $465\ \text{nm}$ LED lamp (irradiance: $65\ \text{mW}/\text{cm}^2$).

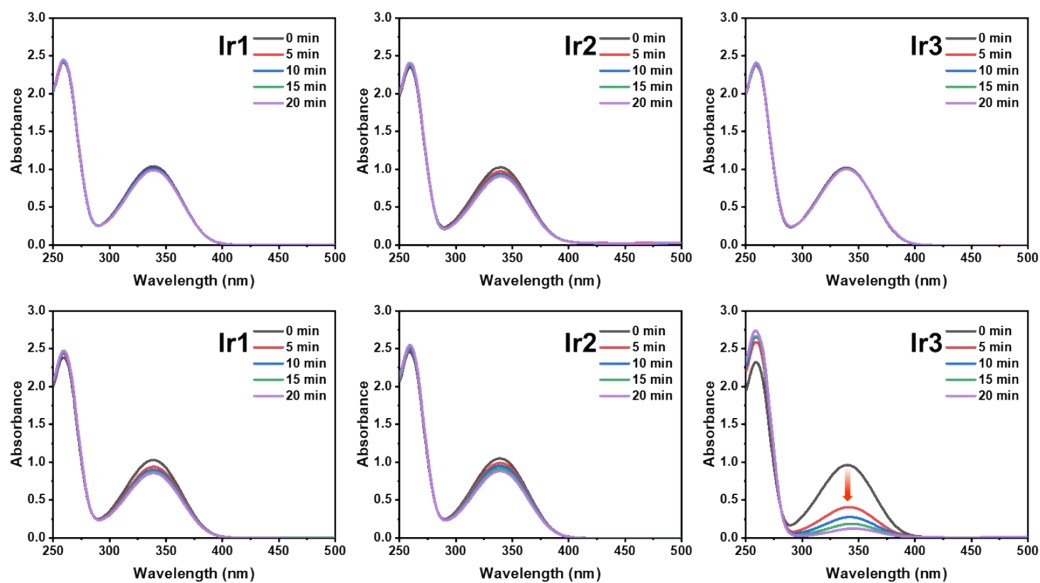


Fig. S16. UV-Vis spectra showing the photocatalytic oxidation of NADH (160 μM) by complexes (5 μM) in PBS. Top: Dark. Bottom: White light LED lamp (irradiance: 14.3 mW/cm^2).

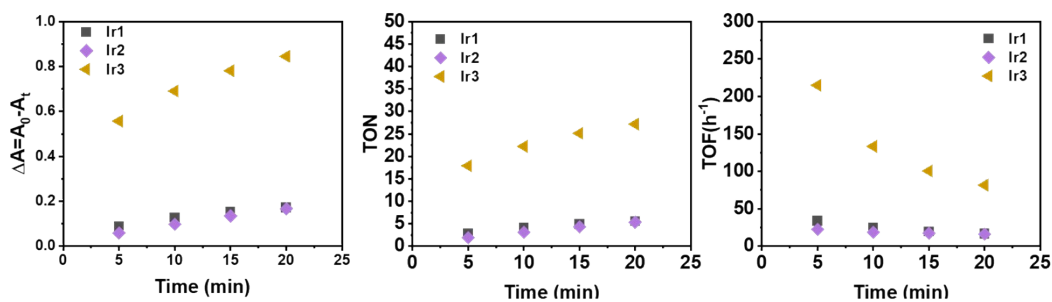


Fig. S17. The ΔA , Turnover number (TON) and **turnover frequency (TOF)** of Ir(III) complexes (5 μM) for NADH (160 μM) photo-oxidation after 20 min of light irradiation. Condition: White light LED lamp (irradiance: 14.3 mW/cm^2).

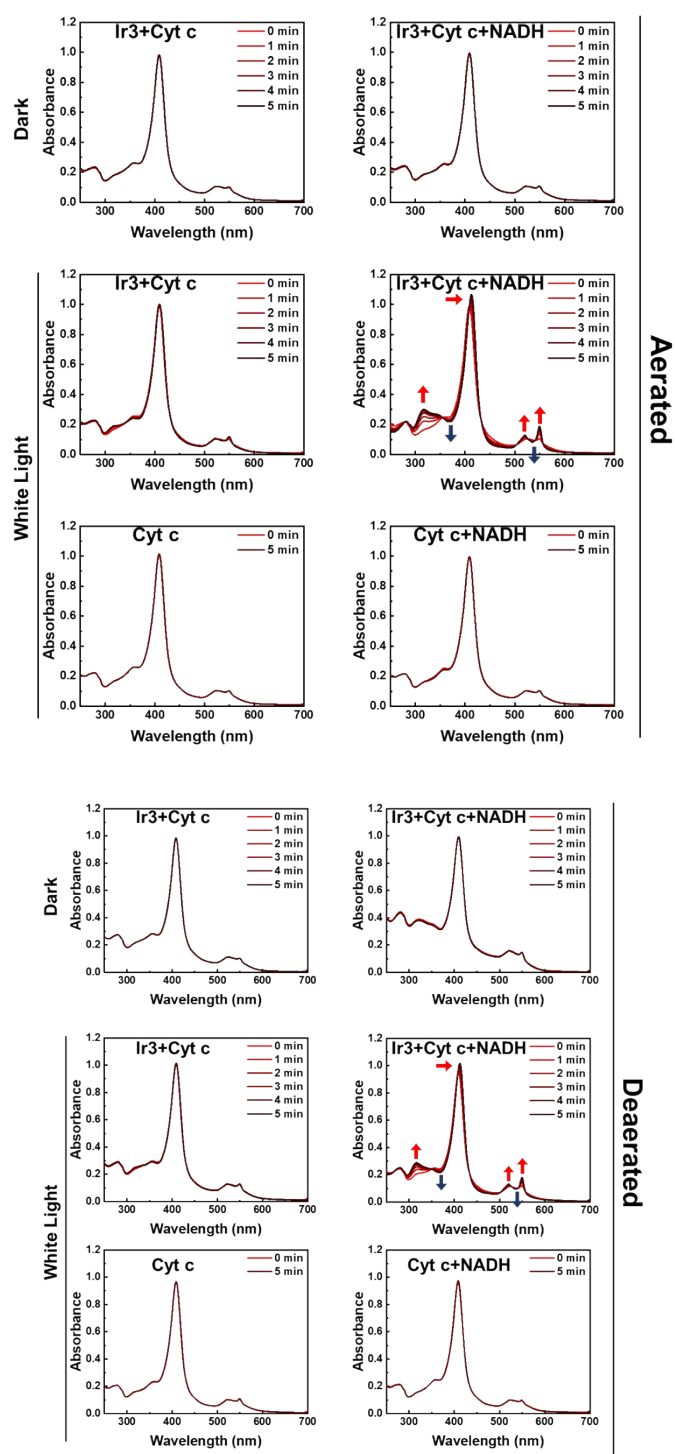


Fig. S18. Photocatalytic reduction of oxidized Fe^{3+} -cyt c (11.2 μM) by NADH (50 μM) and Ir^3 (5 μM) under various conditions. Light irradiation: white light (14.3 mW/cm^2).

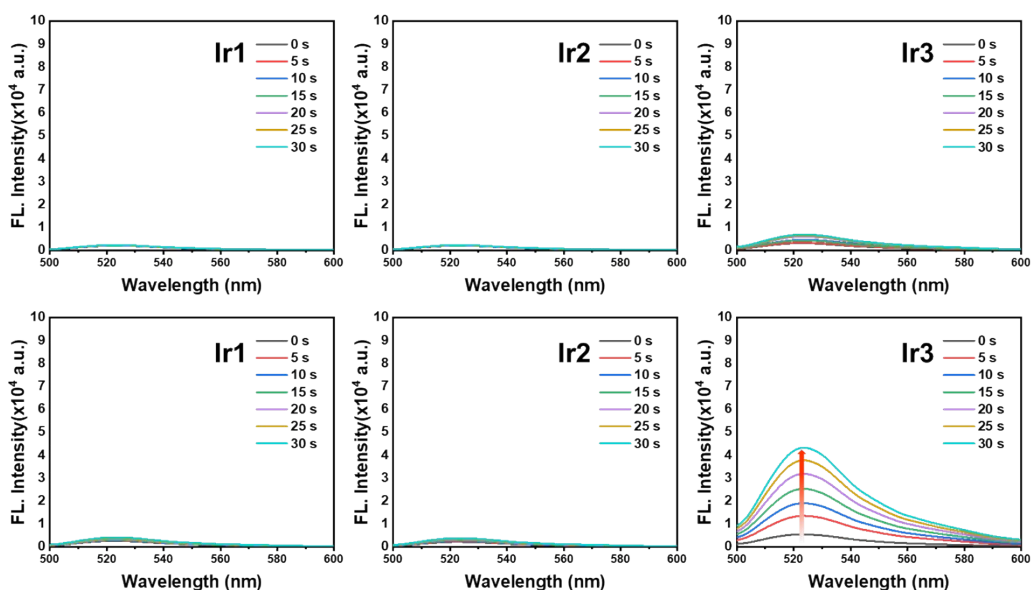


Fig. S19. Determination of $O_2^{\cdot -}$ generation by complexes via monitoring the time-dependent FL emission spectra ($Ex=465$ nm) of DHR123 ($5 \mu M$) after treatment with Ir(III) complexes ($5 \mu M$). Top: Dark. Bottom: White light LED lamp (irradiance: 14.3 mW/cm^2).

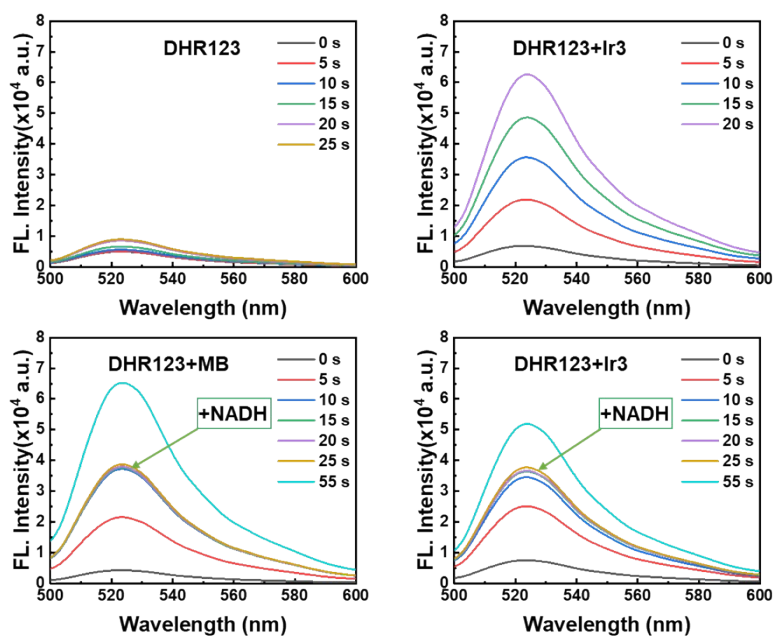


Fig. S20. $O_2^{\cdot -}$ generation was inhibited in the presence of NADH ($5 \mu M$) via monitoring the time-dependent emission spectra ($Ex=465$ nm) of DHR123 ($5 \mu M$) in the presence of Ir3 ($5 \mu M$). Condition: White light LED lamp (irradiance: 14.3 mW/cm^2).

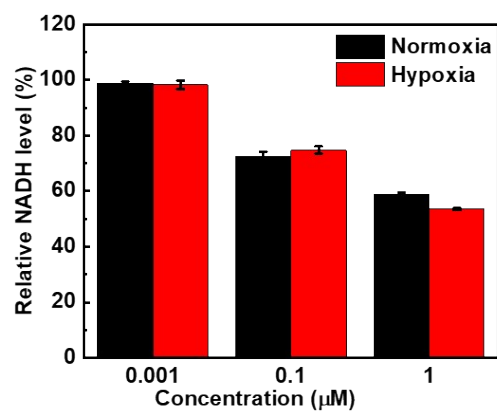


Fig. S21. Relative intracellular NADH levels of A549/DDP cells treated with Ir3 with irradiation (white light, 11.7 J/cm²).

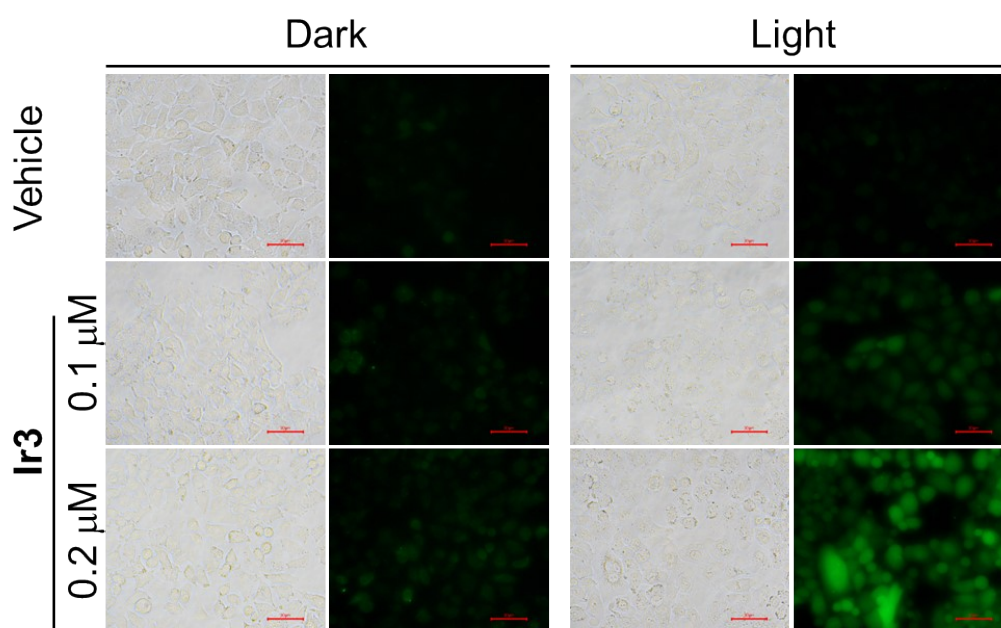


Fig. S22. Intracellular generation of Reactive Oxygen Species (ROS) in A549/DDP cells induced by Ir3 using DCFH-DA probe. scale bar: 50 μm. Condition: white light LED lamp (irradiance: 17.2 J/cm²).

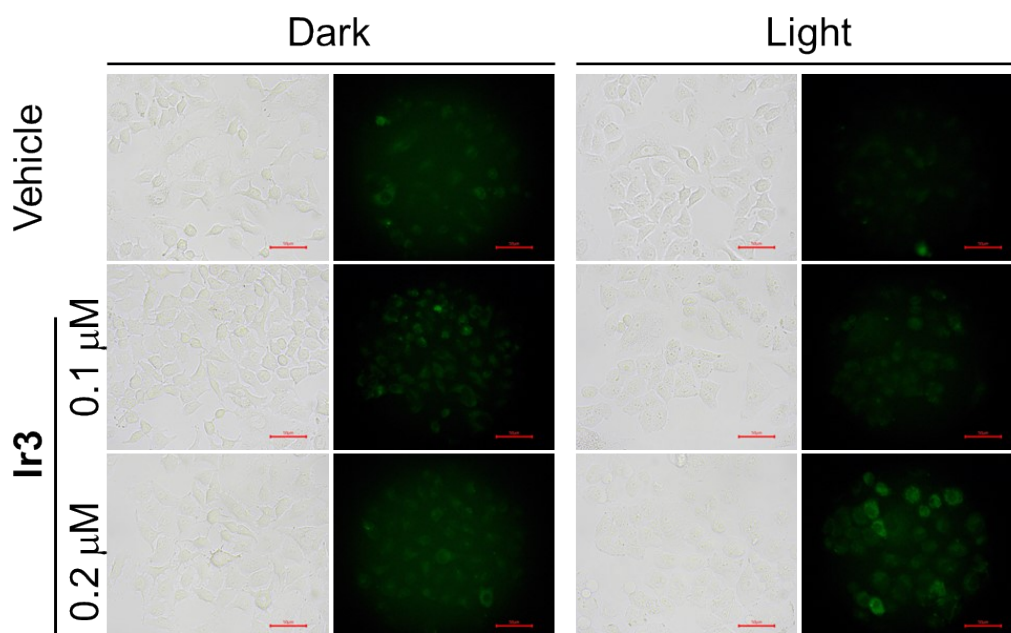


Fig. S23. Intracellular generation of Singlet Oxygen ($^1\text{O}_2$) in A549/DDP cells, induced by Ir3 using SOSG probe. scale bar: 50 μm . Condition: White light LED lamp (irradiance: 17.2 J/cm^2).

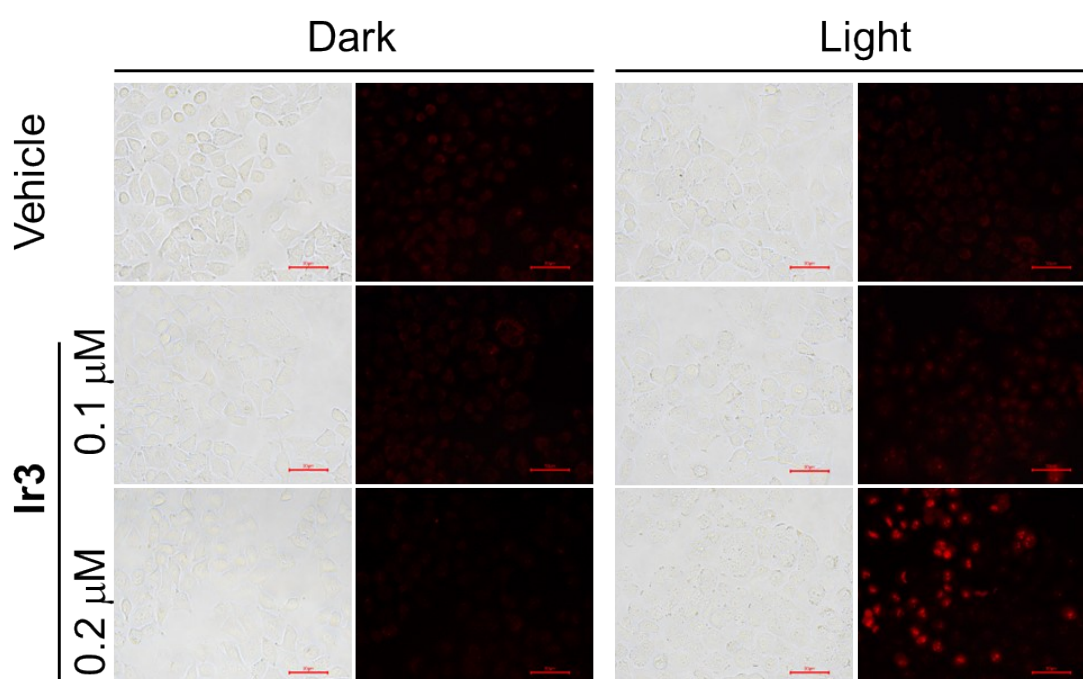


Fig. S24. Intracellular generation of superoxide radicals ($\text{O}_2^{\cdot-}$) in A549/DDP cells induced by Ir3 using DHE probe. scale bar: 50 μm . Condition: white light LED lamp (irradiance: 17.2 J/cm^2).

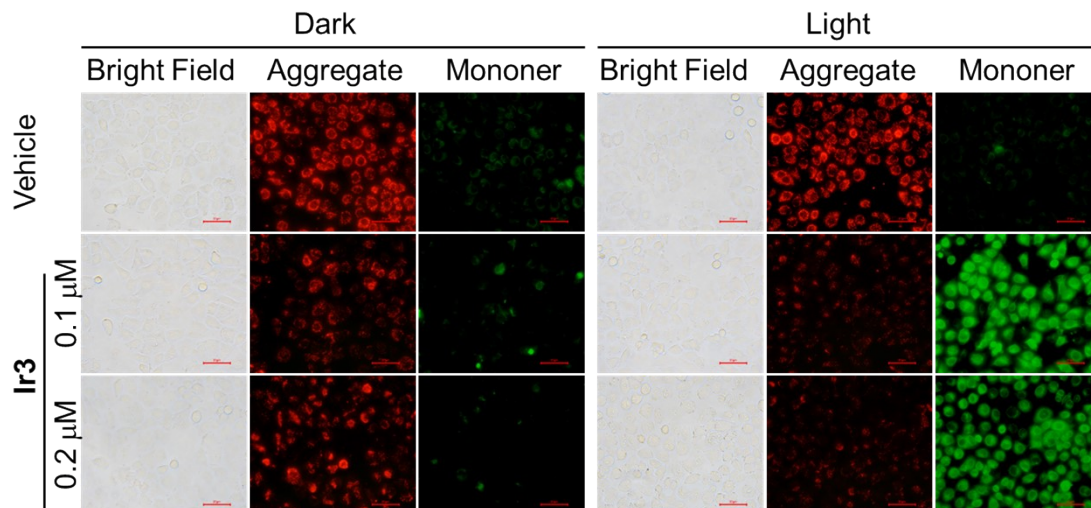


Fig. S25. Variation in the mitochondrial membrane potential(MMP) in A549/DDP cells by Ir3 in the dark or on light treatment, scale bar: 50 μm. Condition: white light LED lamp (irradiance: 17.2 J/cm²).

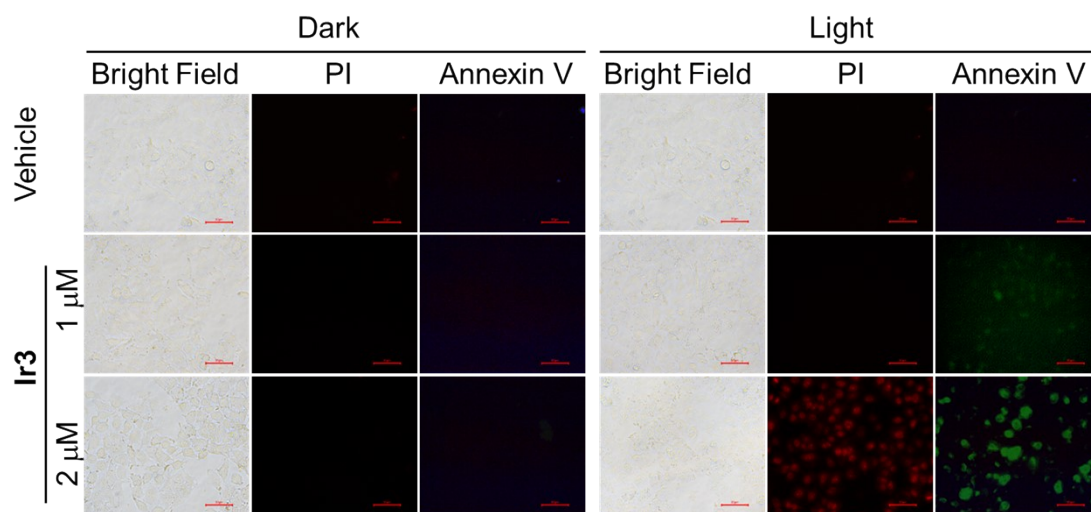


Fig. S26. Photo-induced necro-apoptotic death of A549/DDP cells by Ir3 from Annexin V/PI staining, scale bar: 50 μm. Condition: white light LED lamp (irradiance: 17.2 J/cm²).

References

- 1 L. Philippe, B. Fethi, O. Philippe and M. Vale'rie, *J. Am. Chem. Soc.*, 2002, **124**, 1364-1377.
- 2 H. Ishidaa, S. Tobitab, Y. Hasegawac, R. Katohd and K. Nozakie, *Coord. Chem. Rev.*, 2010, **254**, 2449-2458.
- 3 J. Arden, G. Deltau, V. Huth, U. Kringel, D. Peros and K. Drexhage, *J. Lumin.*, 1991, **48**, 352-358.
- 4 C. Lia, Y. Wang, Y. Lu, J. Guo, C. Zhu, H. He, X. Duan, Mei Pan and C. Su, *Chin. Chem. Lett.*, 2020, **31**, 1183-1187.
- 5 H. Huang, S. Banerjee, K. Qiu, P. Zhang, O. Blacque, T. Malcomson, M. Paterson, G. Clarkson, M. Staniforth, V. Stavros, G. Gasser, H. Chao and P. Sadler, *Nat. Chem.*, 2019, **11**, 1041-1048.